applied sciences

MDPI

Article

A New Kinematic Model of Portable Articulated Coordinate Measuring Machine

Hui-Ning Zhao, Lian-Dong Yu *, Hua-Kun Jia, Wei-Shi Li and Jing-Qi Sun

School of Instrument Science and Opto-electric Engineering, Hefei University of Technology, Hefei 230009, China; hnzhao@mail.hfut.edu.cn (H.-N.Z.); huakun_jia@mail.hfut.edu.cn (H.-K.J.); weishili@hfut.edu.cn (W.-S.L.); aqwsxz123456a@163.com (J.-Q.S.)

* Correspondence: liandongyu@hfut.edu.cn; Tel.: +86-138-5606-1480

Academic Editors: Kuang-Cha Fan and Chien-Hung Liu
Received: 31 March 2016; Accepted: 14 June 2016; Published: 1 July 2016

Abstract: Portable articulated coordinate measuring machine (PACMM) is a kind of high accuracy coordinate measurement instrument and it has been widely applied in manufacturing and assembly. A number of key problems should be taken into consideration to achieve the required accuracy, such as structural design, mathematical measurement model and calibration method. Although the classical kinematic model of PACMM is the Denavit-Hartenberg (D-H) model, the representation of D-H encounters the badly-conditioned problem when the consecutive joint axes are parallel or nearly parallel. In this paper, a new kinematic model of PACMM based on a generalized geometric error model which eliminates the inadequacies of D-H model has been proposed. Furthermore, the generalized geometric error parameters of PACMM are optimized by the Levenberg-Marquard (L-M) algorithm. The experimental result demonstrates that the measurement of standard deviation of PACMM based on the generalized geometric error model has been reduced from 0.0627 mm to 0.0452 mm with respect to the D-H model.

Keywords: portable articulated coordinate measuring machine; generalized geometric error parameters; sample strategy; Levenberg-Marquard algorithm

---

1. Introduction

The portable articulated coordinate measuring machine (PACMM) is a kind of high accuracy coordinate measurement instrument and has the advantages of flexibility, lightweight, portability and easy use compared to the traditional orthogonal CMM. It has been widely applied in manufacturing, assembly [1], *in-situ* measurement, reverse engineering and calibration [2,3]. Error sources of PACMM include structural parameters errors, joint errors, link deflections, thermal deformations and so on. The measurement accuracy of PACMM depends on the proper kinematic model which considers both geometric and non-geometric errors.

Many methods have been proposed in the literatures to establish the kinematic model of robot or PACMM. The Denavit-Hartenberg (D-H) [4] formulation is regarded as the most classical kinematic model for a robot or PACMM. A modified four-parameter D-H formulation [5,6] has been proposed to overcome the badly-conditioned problems when the two adjacent joint axes are parallel or nearly parallel. Reference [7] also showed that another type of the modified D-H formulation which the standard D-H conventions post-multiplies the rotation term around Y-axis could improve the badly-conditioned problem when the two adjacent joint axes are parallel or nearly parallel. In order to meet the three principles of the kinematic model of the manipulator—parametric, continuity and completeness, references [8,9] proposed a complete, parametrically and continuous kinematic model by adding two parameters to Roberts' line parameters. Recently, some researchers also proposed the generalized geometric error model method considering both geometric and non-geometric errors.

For example, reference [10] introduced the generalized geometric error parameters for eliminating the geometric and non-geometric errors and improving the positioning accuracy of the patient positioning system. A general approach for error model of machine tools [11] has been introduced to eliminate the geometric and non-geometric errors of machine tools.

The calibration technique of kinematic structural parameters has also been considered as an efficient method of eliminating geometric and non-geometric errors of CMM, PACMM, machine tools, *etc.* According to performance tests of PACMM [12–14], it is required to calibrate the measurement volume of PACMM by using a 1D standard gauge. Reference [15] introduced a simple artifact with two spheres for the kinematic structural parameters calibration of PACMM. The center distance between two spheres in the artifact was calculated by fitting the central points of two spheres. Reference [16] reported 1D ball bar array. The central points of two spheres were measured by PACMM with the special rigid probe. Reference [17] presented a new full pose measurement method for the kinematic structural parameters calibration of the serial robot. This approach was achieved by an analysis of the features of a set of target points on circular trajectory. Kovač *et al.* [18] developed a high accuracy measurement device based on laser interferometer combining with 1D translation table for calibration and verification of PACMM. Shimojima *et al.* [19] presented a 3D ball plate with nine balls. Piratelli *et al.* [20] introduced the development of virtual ball bar to evaluate the performance of PACMM. González *et al.* [21] introduced a virtual circle gauge was applied in evaluating the performance of PACMM and it was composed of bar gauges of 1000 mm length with four groups of three cone-shaped holes. The above-mentioned virtual geometric gauges are applied to reduce the number of test positions, avoid the measurement points randomly sampled on the virtual geometrical gauges surfaces according to the norms and improve the efficiency of verification procedure for PACMM. Acero *et al.* [22] presented an indexed metrology platform combined with a calibrated ball bar gauge, which was applied in evaluating the performance of PACMM. A simplified and low-price length gauge [23] was applied in calibrating the kinematic structural parameters of PACMM and it had three degrees of freedom (DOFs) and a coefficient of low-thermal expansion.

Besides, calibration algorithm of the robot or PACMM plays a crucial role in improving the measurement accuracy of PACMM. D-H conventions of the measuring arm were improved by Genetic Algorithm (GA) [24]. Although GA had good global search ability during the optimization process of D-H parameters of PACMM, it also had poor local search ability. The kinematic structural parameters of parallel dual-joint CMM were calibrated by using Particle Swarm Optimization (PSO) algorithm [25]. Compared with GA, in most cases, all the particles of PSO may converge to the optimal solution more quickly, but it also may be easy to fall into local optimum. Gao *et al.* [26] proposed a modified Simulated Annealing (SA) algorithm for identifying the structural parameters of PACMM. To overcome the disadvantages of the above-mentioned algorithms which have slow converge rate, the nonlinear least square method [27] has been adopted to calibrate the geometric errors of flexible coordinate measuring robot and compensate its geometric errors. The L-M algorithm proposed by Levenberg and Marquardt [28,29] can improve the disadvantages of the nonlinear least-square method by over-relying on the initial values and having high converge rate. Therefore, L-M algorithm is selected as the calibration algorithm of the generalized geometric error parameters of PACMM.

2. Model

The measurement model aims to establish the transformation relationship between the base frame and the center of the probe, and the model includes the nominal geometric parameters, geometric and non-geometric errors. D-H conventions and generalized geometric error theory are applied in establishing the kinematic model of PACMM, respectively.

2.1. D-H Conventions

D-H conventions is supposed to as the most classical kinematic model method for a robot or PACMM. The transformation matrix A_i from the coordinate frame "$i-1$" to "i" with D-H conventions is indicated by Equation (1):

$$A_i = \begin{bmatrix} cos\theta_i & -sin\theta_i cos\alpha_i & sin\theta_i sin\alpha_i & l_i cos\theta_i \\ sin\theta_i & cos\theta_i cos\alpha_i & -cos\theta_i sin\alpha_i & l_i sin\theta_i \\ 0 & sin\alpha_i & cos\alpha_i & d_i \\ 0 & 0 & 0 & 1 \end{bmatrix} \quad (1)$$

where θ_i, l_i, α_i and d_i denote the joint angle, link length, twist angle, joint offset, respectively.

2.2. Generalized Geometric Error Theory

To describe the kinematic model of PACMM, the transformation matrix of the coordinate frame f_i^{ideal} with respect to f_{i-1}^{real} is indicated by using D-H's 4×4 matrix $_i$. Figure 1 shows the transformation relationship between the coordinate frame f_{i-1}^{real} and f_i^{real}. However, the actual geometric parameters of the coordinate frame f_i^{ideal} with respect to f_i^{real} for PACMM exists the slightly deviations from the nominal values because of the existence of machining errors, assembly errors, link deformation and so on. The transformation relationship between the coordinate frame f_i^{ideal} and f_i^{real} is shown in Figure 2. Therefore, the coordinate frame f_{i-1}^{real} transformed to f_i^{real} would need two steps: Firstly, the homogeneous transformation matrix A_i would be obtained by the coordinate frame f_i^{ideal} with respect to f_{i-1}^{real} ; Secondly, the homogeneous transformation matrix E_i would be obtained by the coordinate frame f_i^{real} with respect to f_i^{ideal}. Equation (2) follows:

$$E_i = Rot\,(x_i, \varepsilon_{i4})\;Rot\,(y_i, \varepsilon_{i5})\;Rot\,(z_i, \varepsilon_{i6})\;Trans\,(\varepsilon_{i1}, \varepsilon_{i2}, \varepsilon_{i3}) \quad (2)$$

where the three parameters $\varepsilon_{i1}, \varepsilon_{i2}, \varepsilon_{i3}$ indicate the translation values from the origin O_i^{ξ} to $O_i^{\Re}$ in the frame f_i^{ideal} along the X, Y and Z axes, respectively. The other three parameters $\varepsilon_{i4}, \varepsilon_{i5}, \varepsilon_{i6}$ represent the Euler angles of the coordinate frame f_i^{real} with respect to f_i^{ideal} in the Figure 2.

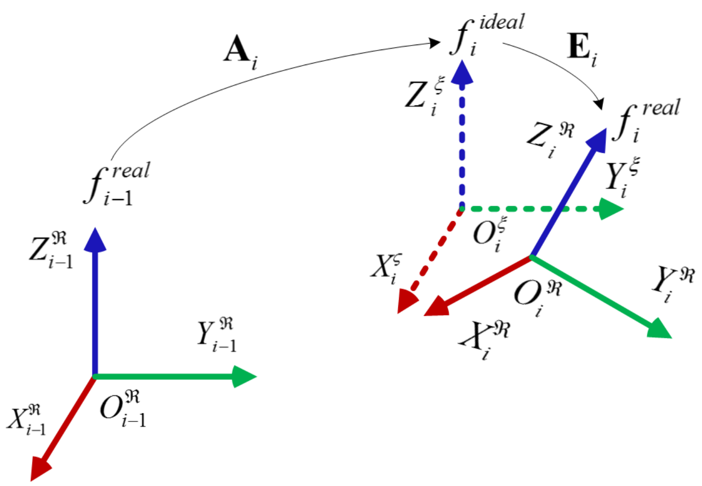

Figure 1. Frame translation and rotation due to the errors for the i^{th} link.

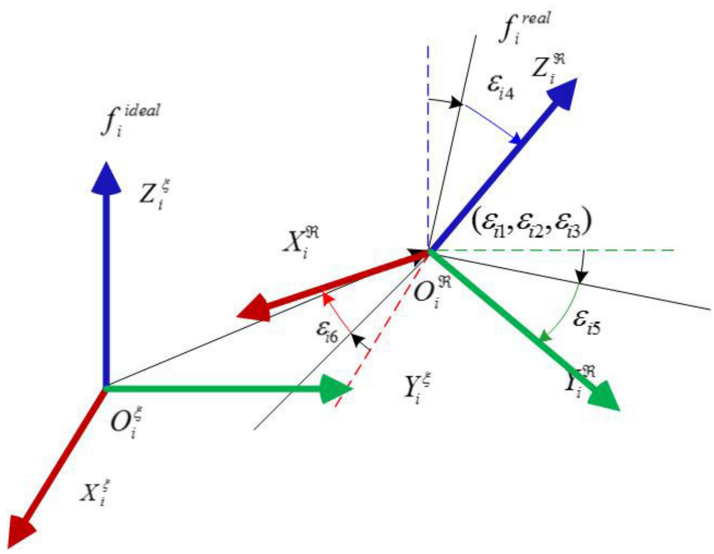

Figure 2. Definition of the generalized geometric error parameter for the i^{th} link.

In the Equation (2), the six parameters $\varepsilon_{i1}, \varepsilon_{i2}, \varepsilon_{i3}, \varepsilon_{i4}, \varepsilon_{i5}, \varepsilon_{i6}$ are generally called the generalized geometric error parameters. To simplify the calculation process, the matrix E_i is approximately represented by the Taylor's formula expansion of the Equation (2). The first order values of expansion formula only remain because the coordinate frame f_i^{real} slightly deviates from f_i^{ideal}. Therefore, the matrix E_i is rewritten as the Equation (3):

$$E_i = \begin{bmatrix} 1 & -\varepsilon_{i6} & \varepsilon_{i4} & \varepsilon_{i1} \\ \varepsilon_{i6} & 1 & -\varepsilon_{i5} & \varepsilon_{i2} \\ -\varepsilon_{i4} & \varepsilon_{i5} & 1 & \varepsilon_{i3} \\ 0 & 0 & 0 & 1 \end{bmatrix} \quad (3)$$

The matrix B_i called the generalized geometric error matrix and indicates the transformation matrix of the coordinate frame f_i^{real} with respect to f_{i-1}^{real}.

$$B_i = A_i E_i \quad (4)$$

2.3. Kinematic Model Based on Generalized Geometric Error Theory

There are two steps for establishing the kinematic model of PACMM. Firstly, each joint variable of PACMM is nominally equal to zero at the initial state. In other words, this state is also called the zero pose. Secondly, the kinematic model of PACMM would be established by the generalized geometric error matrix at the initial state. In Figure 3, the homogeneous matrix A_i is obtained by the coordinate frame $O_{i-1}^{\Re} X_{i-1}^{\Re} Y_{i-1}^{\Re} Z_{i-1}^{\Re}$ transformed to $O_i^{\xi} X_i^{\xi} Y_i^{\xi} Z_i^{\xi}$, and the matrix E_i represents the coordinate frame $O_i^{\Re} X_i^{\Re} Y_i^{\Re} Z_i^{\Re}$ slightly deviating from the ideal frame $O_i^{\xi} X_i^{\xi} Y_i^{\xi} Z_i^{\xi}$. When $i = 0,7$ the corresponding frames are the base frame and the center of the rigid probe of PACMM, respectively. It is worth noting that the coordinate frame is not directly established by the D-H model method because there is not the rotation joint at the coordinate frame $O_6^{\Re} X_6^{\Re} Y_6^{\Re} Z_6^{\Re}$. The point P indicates the center of the probe here. Therefore, the coordinate frame is established by the following method: The projective point P' is obtained by the point P projective to the plane of $X_5^{\Re} O_5^{\Re} Z_5^{\Re}$, and the line PP' is in line with the $Z_6^{\Re}$ axis of the coordinate frame. Therefore, the coordinate frame $O_6^{\Re} X_6^{\Re} Y_6^{\Re} Z_6^{\Re}$ is established by the above method in Section 2.2. The coordinate frame $O_7^{\Re} X_7^{\Re} Y_7^{\Re} Z_7^{\Re}$ is obtained by the translation d_7 along the axis in the coordinate frame $O_6^{\Re} X_6^{\Re} Y_6^{\Re} Z_6^{\Re}$. However, the angular encoder includes zero position error at the zero position because of the manufacture and assembly errors of the angular encoder. θ_{i0} is supposed to represent the zero position error of the joint variable θ_i at the initial zero position. Then, the actual joint variable is indicated by $\Theta_i = \theta_{i0} + \theta_i$. The transformation matrix A_i is rewritten as the Equation (5):

$$A_i = \begin{bmatrix} cos\Theta_i & -sin\Theta_i cos\alpha_i & sin\Theta_i sin\alpha_i & l_i cos\Theta_i \\ sin\Theta_i & cos\Theta_i cos\alpha_i & -cos\Theta_i sin\alpha_i & l_i sin\Theta_i \\ 0 & sin\alpha_i & cos\alpha_i & d_i \\ 0 & 0 & 0 & 1 \end{bmatrix} \quad (5)$$

Therefore, the relationship matrix T from the base frame $O_0^{\Re} X_0^{\Re} Y_0^{\Re} Z_0^{\Re}$ to the probe frame $O_7^{\Re} X_7^{\Re} Y_7^{\Re} Z_7^{\Re}$ is represented by the Equation (6):

$$T = \prod_{i}^{6} B_i Trans\,(0, 0, d_7) = \prod_{i}^{6} A_i E_i Trans\,(0, 0, d_7) \quad (6)$$

where all the generalized geometric error parameters are indicated by using vector $\varepsilon = \left[\varepsilon_{11}, \varepsilon_{12}, \cdots, \varepsilon_{ij}, \cdots, \varepsilon_{66}\right]$ $(i, j = 1, 2, \cdots, 6)$ in the actual kinematic model of PACMM.

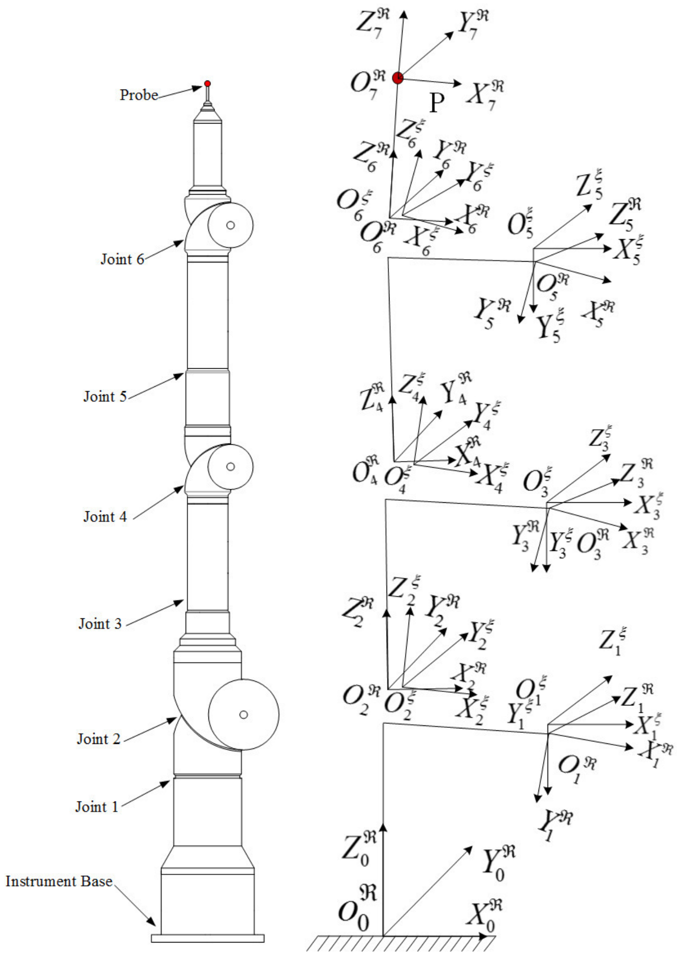

Figure 3. Configuration of portable articulated coordinate measuring machine (PACMM) based on the generalized geometric error model.

3. Error Model and Calibration Algorithm

3.1. Error Model

To ensure the high accuracy measurement results of PACMM, the generalized geometric error parameters vector of Equation (6) must be accurately calibrated except for the nominal values $\theta_{i0}, \alpha_i, l_i, d_i\ (i = 1, 2, \cdots, 6)$ and d_7. In this paper, an Invar length gauge which has the coefficient of low-thermal expansion is employed as the gauge for calibrating the generalized geometric error parameters of PACMM. For ease of use the Invar length gauge is placed on the three DOFs support platform shown in Figure 4. The pose of the Invar length gauge with regard to PACMM is changed by rotating the three DOFs support platform to collect six joint angle values of PACMM in different poses. The Invar length gauge has three cone-shaped holes on one surface, the length between cone-shaped hole 1 and 2 is $L_{12} = 514.371$ mm and the length between cone-shaped hole 1 and 3 is $L_{13} = 1015.962$ mm. In this paper, L_{12} is selected as the standard value for calibrating the generalized geometric error parameters of PACMM. Therefore, the error model of the generalized geometric error parameters of PACMM is established based on the spatial distance. The measuring points P_k^1 and P_k^2 are obtained when the probe is placed in cone-shaped hole 1 and 2, respectively. Therefore, the error model of PACMM is indicated by Equation (7):

$$E_k(\varepsilon) = L_{12} - \|P_k^1 - P_k^2\| \tag{7}$$

where the symbol $\|\bullet\|$ indicates the norm of the vector. k indicates the serial number of measurement points.

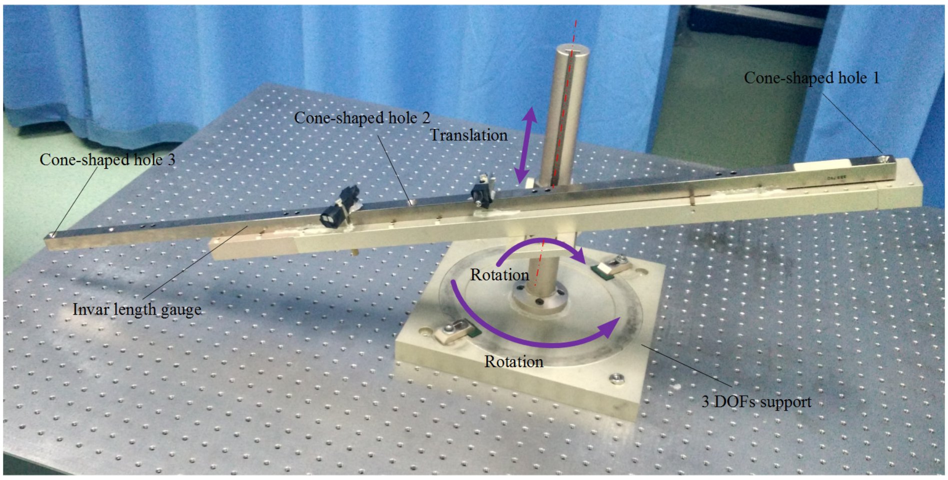

Figure 4. Length gauge.

According to the least square principle, the objective function is established by Equation (8):

$$F(\varepsilon) = \sum_{k=1}^{m} E_k^2(\varepsilon) = \sum_{k=1}^{m} \left(L_{12} - \|P_k^1 - P_k^2\|\right)^2 \tag{8}$$

where m indicates the number of measurement points.

3.2. Calibration Algorithm

Calibration algorithm is supposed to as the main work for solving the generalized geometric error parameters in Equation (8). The selection of calibration algorithm lies in its convergence rate and identification efficiency. Although GA, PSO, modified SA and nonlinear least square method have been applied in calibrating the kinematic parameters of robot or PACMM, the above-mentioned calibration algorithms with respect to LM algorithm have slower convergence rate and poorer stability. Therefore, LM algorithm is selected as the calibration algorithm for calibrating the generalized geometric error parameters of PACMM. Its detailed calculation procedures are as follows:

Step 1: Set the initial estimation values vector $\varepsilon^{(0)}$ of generalized geometric error parameters vector ε, the initial damping factor $\mu = \mu_0^{(0)}$, permissible error $\epsilon > 0$, set the flag of the iteration step $t = 0$ and the growth factor $\nu > 0, \nu = 2, 5$ or 10;

Step 2: Calculate $E^{(t)} = E(\varepsilon^{(t)})$, $S^{(t)} = E^{(t)T}E^{(t)}$, $J^{(t)} = \left[\dfrac{\partial E_k^{(t)}(\varepsilon^{(t)})}{\partial \varepsilon_{ij}}\right]$, $(t = 1, 2, \cdots, n)$;

Step 3: Solve $(J^{(t)T}J^{(t)} + \mu^{(t)}I)\Delta\varepsilon^{(t)} = -J^{(t)T}E^{(t)}$;

Step 4: Calculate $\varepsilon^{(t+1)} = \varepsilon^{(t)} + \Delta\varepsilon^{(t)}$, $E^{(t+1)} = E(\varepsilon^{(t+1)})$, $S^{(t+1)} = E^{(t+1)T}E^{(t+1)}$;

Step 5: If $\|\Delta\varepsilon^{(t)}\| < \epsilon$, vector $\varepsilon^{(t)}$ is supposed to as the best estimate ε^*, else $t = t + 1$;

Step 6: If $S^{(t+1)} < S^{(t)}$, then $\mu^{(t+1)} = \mu^{(t)}/\nu$, go to Step 2, else $\mu^{(t+1)} = \mu^{(t)}\nu$, go to Step 3.

However, some generalized geometric error parameters resulting in the tiny contributions for the probe position errors of PACMM could not be calibrated. Therefore, these parameters are assimed to be the redundant parameters of generalized geometric error parameters for error model of PACMM. The redundant parameters $\varepsilon_{21}, \varepsilon_{31}, \varepsilon_{32}, \varepsilon_{34}, \varepsilon_{35}, \varepsilon_{41}, \varepsilon_{46}, \varepsilon_{51}, \varepsilon_{52}, \varepsilon_{66}$ are eliminated by using the analysis method introduced by Zhang *et al.* [30].

4. Sample Strategy

In fact, The sampling process for calibration data of PACMM records its six joint values. The calibration accuracy of PACMM must be affected by the sampling randomness in the whole work volume of PACMM. Borm *et al.* [31] introduced an optimized sampling strategy for calibrating the serial robot, needs the joint values of the serial robot collected uniformly in the corresponding joint spaces. Therefore, the length gauge should be uniformly distributed in the whole work volume of PACMM for sampling the calibration data to reduce the sampling randomness of the PACMM. However, the partial work volume of PACMM can not be collected according to performance tests of PACMM. The length gauge is uniformly distributed at four different positions around the PACMM. The length gauge can be uniformly rotated by the different poses to reduce the geometric and non-geometric errors of PACMM according to the Figure 5.

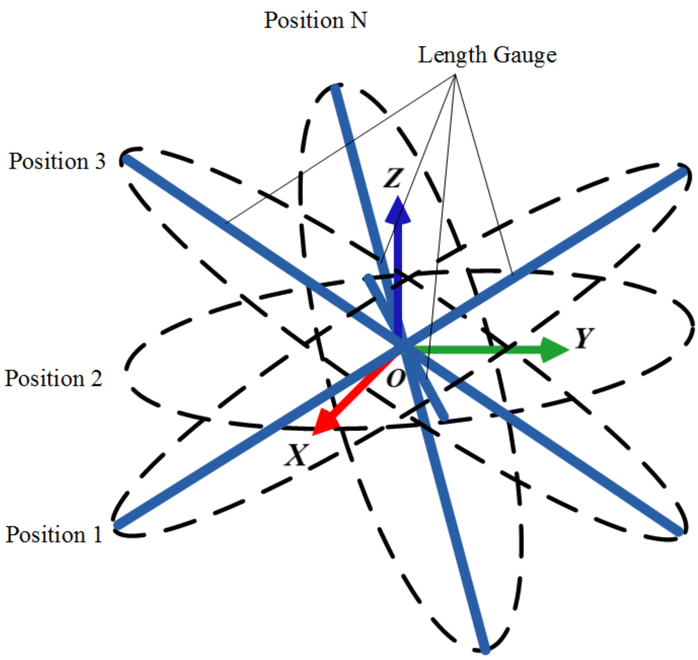

Figure 5. Sample strategy.

The detailed sampling procedures are shown in the Figure 6.

Figure 6. Sampling procedure.

5. Experiment

In this section, the generalized geometric error parameters calibration of PACMM is performed by L-M algorithm in the Section 3.2. In order to verify the advantage of the proposed method with respect to D-H model [32], the comparison experiment is also done by PACMM based on the generalized geometric error parameters and D-H model, respectively.

5.1. Calibration

The nominal values of the kinematic structural parameters of the kinematic model of PACMM are listed in the Table 1. The parameter d_7 of the probe is equal to 210 mm here.

Table 1. Nominal values of structural parameters.

Parameters	A_1	A_2	A_3	A_4	A_5	A_6
θ (rad)	0	-1.57	-3.33	-4.57	-0.97	-3.96
α (rad)	$-\pi/2$	$\pi/2$	$-\pi/2$	$\pi/2$	$-\pi/2$	$\pi/2$
l (mm)	40	-40	32	-32	32	-32
d (mm)	0	0	440	0	340	0

In the error model of PACMM, the initial generalized geometric error parameters vector $\varepsilon^{(0)}$ is equal to 0. In the process of the calibration, the length gauge would be placed by the above method in the Section 4. The calibration data are substituted into the L-M algorithm of the Section 3.2. The convergence value of the objective function $F(\varepsilon)$ is 0.1402 by 50 iterations. Figure 7 shows that the value of $F(\varepsilon)$ tends to be stabilized in about five iterations. The generalized geometric error parameter vector ε^* is supposed to as the optimal parameter vector for PACMM. The generalized geometric error parameters calibrated of PACMM are listed in the Table 2.

Table 2. Generalized geometric error parameters calibrated.

Parameters	E_1	E_2	E_3	E_4	E_5	E_6
ε_1 (mm)	−0.0156	−0.0060	−0.0062	−0.0076	0.0164	−0.0038
ε_2 (mm)	-	0.0071	0.0081	−0.0025	0.0204	−0.0017
ε_3 (mm)	-	-	-	-	-	0.0247
ε_4 (rad)	-	0.0015	−0.0307	0.0443	−0.0332	-
ε_5 (rad)	-	0.0288	−0.0423	−0.0318	−0.0013	-
ε_6 (rad)	−0.0011	−0.0021	0.0021	−0.0007	0.0018	-

- Redundant parameter.

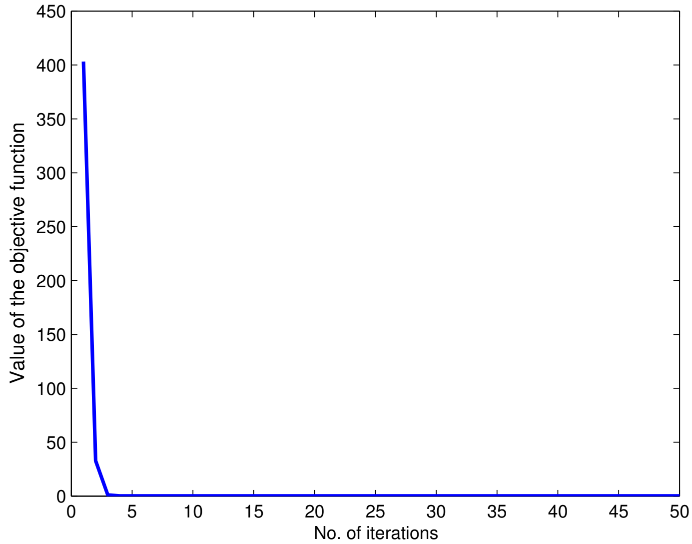

Figure 7. Convergence curve.

The measurement errors of the length gauge using PACMM before and after calibrating 50 times are shown in the Figure 8. In addition, the measurement standard deviation of PACMM for the length gauge is reduced from 0.5550 mm (before calibration) to 0.0452 mm (after calibration).

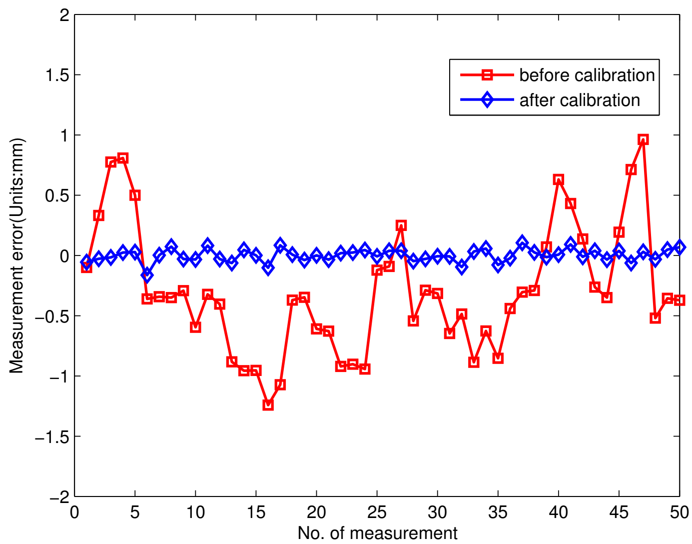

Figure 8. Measurement residual errors of length gauge using PACMM before and after calibration.

5.2. Comparison

To verify the advantage of the kinematic model of PACMM based on generalized geometric error model with respect to D-H model, this paper presents that PACMM measures the length gauge 20 times at four different positions and the measured angle data is calculated by generalized geometric error parameters and D-H method, respectively. Figure 9 shows the measurement standard deviations of length gauge using PACMM based on D-H and generalized geometric error method at four different positions. Besides, the results of the comparison experiment demonstrate that the measurement standard deviation of length gauge using PACMM based on the generalized geometric error method is reduced from 0.0627 mm to 0.0452 mm with respect to the D-H model.

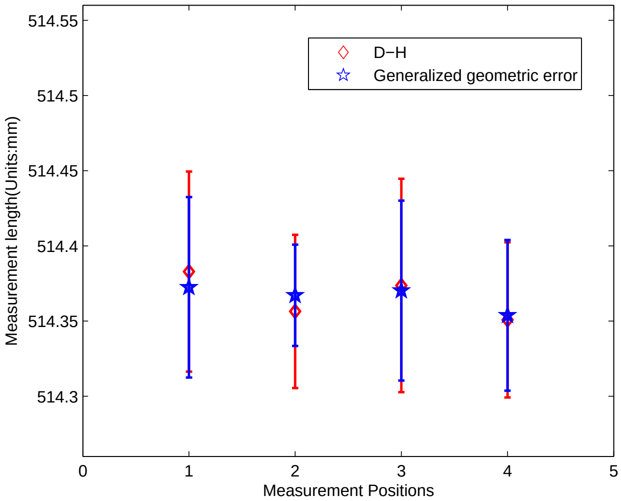

Figure 9. Comparison of the measurement results of length gauge using PACMM based on the Denavit-Hartenberg (D-H) and generalized geometric error method.

6. Discussion

The comparison experimental results demonstrate that the proposed method is effective and the higher measurement accuracy of PACMM using the proposed method could be achieved with respect to D-H model. Note here that the measurement accuracy of FaroArm Platinum 1.8 m is 0.037 mm, as specified by ASME B89.4.22 norm. The measurement accuracy of PACMM using the proposed method is slightly lower than Faro Platinum 1.8 m, but its price is only half of the FaroArm Platinum 1.8 m. In future work, improving the manufacturing process of parts, optimizing the calibration method of the structural parameters, reducing the number of PACMM DOFs in the process of the practical work and adopting multi-group kinematic parameters calibrated for the kinematic model of PACMM would be regarded as the research key to improving the measurement accuracy of PACMM.

7. Conclusions

A new kinematic model of PACMM which considers both geometric and non-geometric errors is proposed on the basis of generalized geometric error model in this paper. Generalized geometric error parameters are calibrated by the L-M algorithm. The experimental results demonstrate that the measurement standard deviation of the length gauge is reduced from 0.5550 mm (before calibration) to 0.0452 mm (after calibration). Besides, the results of the comparison experiment which is also performed to illustrate the advantage of PACMM based on the generalized geometric error method, demonstrate the measurement standard deviation of the proposed method, which is reduced from 0.0627 mm to 0.0452 mm with respect to D-H.

Acknowledgments: This research is supported by National Natural Science Foundation of China (Grant No.: 51375137) and Project 111 (Grant No.: B12019) and National Key Scientific Apparatus Development Project (Grant No.: 2013YQ220893). The authors would like to thank all other members of the research team for their contributions to this research.

Author Contributions: Hui-ning Zhao, Lian-dong Yu and Wei-shi Li conceived and designed the experiments and wrote the paper; Hua-kun Jia performed the experiments; Hui-ning Zhao and Hua-kun Jia analyzed the data; Jing-qi Sun created the figures.

Conflicts of Interest: The authors declare no conflict of interest.

Abbreviations

The following abbreviations are used in this manuscript:

PACMM	Portable Articulated Coordinate Measuring Machine
CMM	Coordinate Measuring Machine
D-H	Denavit-Hartenberg
L-M	Levenberg-Marquard
1D	one-dimensional
DOF	degree of freedom
GA	Genetic Algorithm
PSO	Particle Swarm Optimization
SA	Simulated Annealing

References

1. Yu, L.D.; Zhao, H.N.; Zhang, W.; Li, W.S.; Deng, H.X.; Song, Y.T.; Gu, Y.Q. Development of precision measurement network of experimental advanced superconducting tokamak. *Opt. Eng.* **2014**, *52*, 26–31.
2. Joubair, A.; Slamani, M.; Bonev, I.A. A novel *XY*-Theta precision table and a geometric procedure for its kinematic calibration. *Robot. Comput.-Integr. Manuf.* **2012**, *28*, 57–65.
3. Chen, I.M.; Yang, G.; Tan, C.T.; Yeo, S.H. Local POE model for robot kinematic calibration. *Mech. Mach. Theory* **2001**, *36*, 1215–1239.
4. Denavit, J.; Hartenberg, R.S. A kinematic notation for lower-pair mechanisms based on matrices. *ASME J. Appl. Mech.* **1955**, *22*, 215–221.
5. Hayati, S.A. Robot arm geometric link parameter estimation. In Proceedings of the 22nd IEEE Conference on Decision and Control, San Antonio, TX, USA, 14–16 December 1983; pp. 1477–1483.
6. Judd, R.P.; Knasinski, A.B. A technique to calibrate industrial robots with experimental verification. *IEEE Trans. Robot. Autom.* **1990**, *6*, 20–30.
7. Veitschegger, W.K.; Wu, C.H. Robot calibration and compensation. *IEEE J. Robot. Autom.* **1988**, *4*, 643–656.
8. Zhuang, H.; Roth, Z.S.; Hamano, F. A complete and parametrically continuous kinematic model for robot manipulators. *IEEE Trans. Robot. Autom.* **1992**, *8*, 451–463.
9. Roth, Z.S.; Mooring, B.; Ravani, B. An overview of robot calibration. *IEEE J. Robot. Autom.* **1987**, *3*, 377–385.
10. Meggiolaro, M.A.; Dubowsky, S.; Mavroidis, C. Geometric and elastic error calibration of a high accuracy patient positioning system. *Mech. Mach. Theory* **2005**, *40*, 415–427.
11. Tian, W.; Gao, W.; Zhang, D.; Huang, T. A general approach for error modeling of machine tools. *Int. J. Mach. Tools Manuf.* **2014**, *79*, 17–23.
12. American Society of Mechanical Engineering (ASME). *Methods for Performance Evaluation of Articulated Arm Coordinate Measuring Machines*; AMSE B89.4.22; American Society of Mechanical Engineering: New York, NY, USA, 2005; pp. 1–45.
13. Verein Deutscher Ingenieure (VDI). *Acceptance and Reverification Test for Articulated Arm Coordinate Measuring Machines*; VDI/VDE 2617 Part 9; Verein Deutscher Ingenieure: Düsseldorf, Germany, 2009; pp. 1–20.
14. International Organization for Standardization. *Geometrical Product Specifications (GPS)—Acceptance and Reverification Tests for Coordinate Measuring Systems (CMS)—Part 12: Articulated Arm Coordinate Measurement Machines (CMM)*; ISO/CD 10360-12; ISO: Geneva, Switzerland, 2014; pp. 1–42.
15. Furutani, R.; Shimojima, K.; Takamasu, K. Kinematical calibration of articulated CMM using multiple simple artifacts. In Proceedings of the 17th IMEKO World Congress, Dubrovnik, Croatia, 22–27 June 2003; pp. 1789–1801.

16. Santolaria, J.; Aguilar, J.J.; Yagüe, J.A.; Pastor, J. Kinematic parameter estimation technique for calibration and repeatability improvement of articulated arm coordinate measuring machines. *Precis. Eng.* **2008**, *32*, 251–268.
17. Nguyen, H.N.; Zhou, J.; Kang, H.J. A new full pose measurement method for robot calibration. *Sensors* **2013**, *13*, 9132–9147.
18. Kovač, I.; Frank, A. Testing and calibration of coordinate measuring arms. *Precis. Eng.* **2001**, *25*, 90–99.
19. Shimojima, K.; Furutani, R.; Takamasu, K.; Araki, K. The estimation method of uncertainty of articulated coordinate measuring. In Proceedings of the 2002 IEEE International Conference on Industrial Technology (IEEE ICIT '02), Bangkok, Thailand, 11–14 December 2002; Volume 1, pp. 411–415.
20. Piratelli-Filho, A.; Lesnau, G.R. Virtual spheres gauge for coordinate measuring arms performance test. *Measurement* **2010**, *43*, 236–244.
21. González-Madruga, D.; Cuesta, E.; Patiño, H.; Barreiro, J.; Martinez-Pellitero, S. Evaluation of AACMM Using the Virtual Circles Method. *Procedia Eng.* **2013**, *63*, 243–251.
22. Acero, R.; Brau, A.; Santolaria, J.; Pueo, M. Verification of an articulated arm coordinate measuring machine using a laser tracker as reference equipment and an indexed metrology platform. *Measurement* **2015**, *69*, 52–63.
23. Li, J.; Yu, L.D.; Sun, J.Q.; Xia, H.J. A Kinematic Model for Parallel-Joint Coordinate Measuring Machine. *J. Mech. Robot.* **2103**, *5*, 044501.
24. Light, T.V.; Gorlach, I.A.; Schönberg, A.; Schmitt, R. Measuring arm calibration. In Proceedings of the 5th European Conference on European Computing Conference, Paris, France, 28–30 April 2011; pp. 222–227.
25. Dong, Z.; Zhang, W.; Zhao, H.N.; Yu, L.D. Structural parameter calibration for parallel dual-joint coordinate measuring machine. *Nanotechnol. Precis. Eng.* **2015**, *13*, 287–292.
26. Gao, G.B.; Wen, W.; Lin, K.; Chen Z.G. Parameter identification based on modified annealing algorithm for articulated arm CMMs. *Opt. Precis. Eng.* **2009**, *17*, 2499–2505.
27. Liu, W.L.; Qu X.H.; Yan, Y.G. Self-Calibration and Error Compensation of Flexible Coordinate Measuring Robot. In Proceedings of the 2007 International Conference on Mechatronics and Automation, Harbin, China, 5–8 August 2007; pp. 2489–2494.
28. Levenberg, K. A Method for the Solution of Certain Non-linear Problems in Least Squares. *Quart. Appl. Math.* **1944**, *2*, 164–168.
29. Marquardt, D.W. An Algorithm for Least Square Estimation of Non-Linear. *J. Soc. Ind. Appl. Math.* **1963**, *11*, 431–441.
30. Zhang, T.; Liang, D.; Dai, X. Test of Robot Distance Error and Compensation of Kinematic Full Parameters. *Adv. Mech. Eng.* **2014**, *6*, 1–9.
31. Borm, J.H.; Menq, C.H. Determination of Optimal Measurement Configurations for Robot Calibration Based on Observability Measure. *Int. J. Robot. Res.* **1991**, *10*, 51–63.
32. Zheng, D.T.; Xiao, Z.Y.; Xia, X. Multiple Measurement Models of Articulated Arm Coordinate Measuring Machines. *Chin. J. Mech. Eng.* **2015**, *28*, 994–998.